Supporting Information

A Three-Dimensional Interconnected Nitrogen-Doped Graphene-Like Porous Carbon-Modified Separator for High-Performance Li-S Batteries

Wen Huang[a], Daqian Ruan[b], Hui Chen[a], Kai Hu[a], Juan Wen[b], Wenqi Yan[b], Yusong Zhu[a], Yi Zhang[a], Nengfei Yu[a,*] and Yuping Wu[a,b,*]

[a] *School of Energy Science and Engineering, Nanjing Tech University, Nanjing 211816, China.*
[b] *Institute of Advanced Materials (IAM), Nanjing Tech University, Nanjing 210009, China*

[*]Corresponding author.
E-mail address: E-mail: yunf@njtech.edu.cn (N. Yu); wuyp@fudan.edu.cn (Y. Wu)

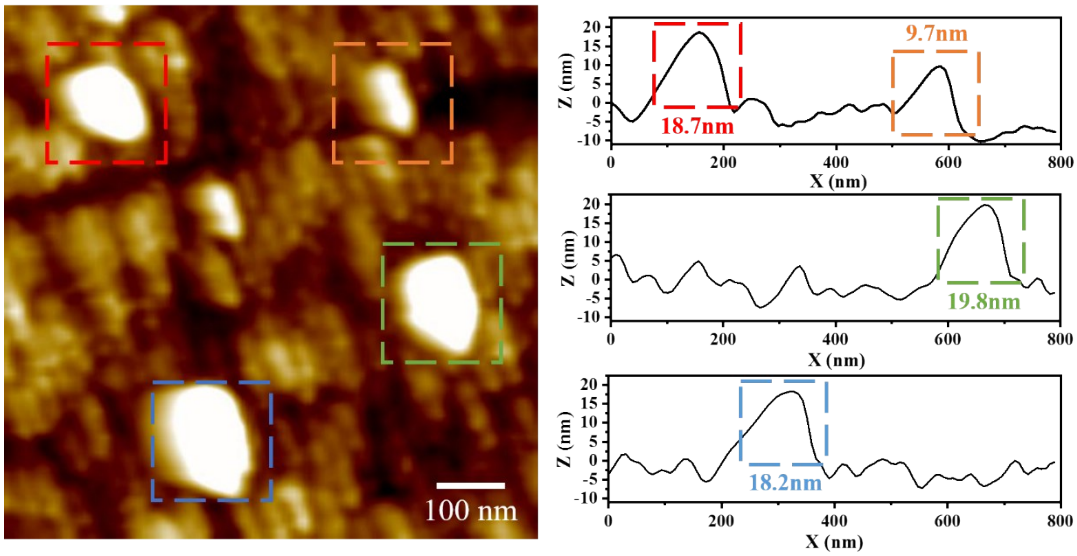

Fig. S1. The atomic force micrograph and thickness distribution of N-GCs.

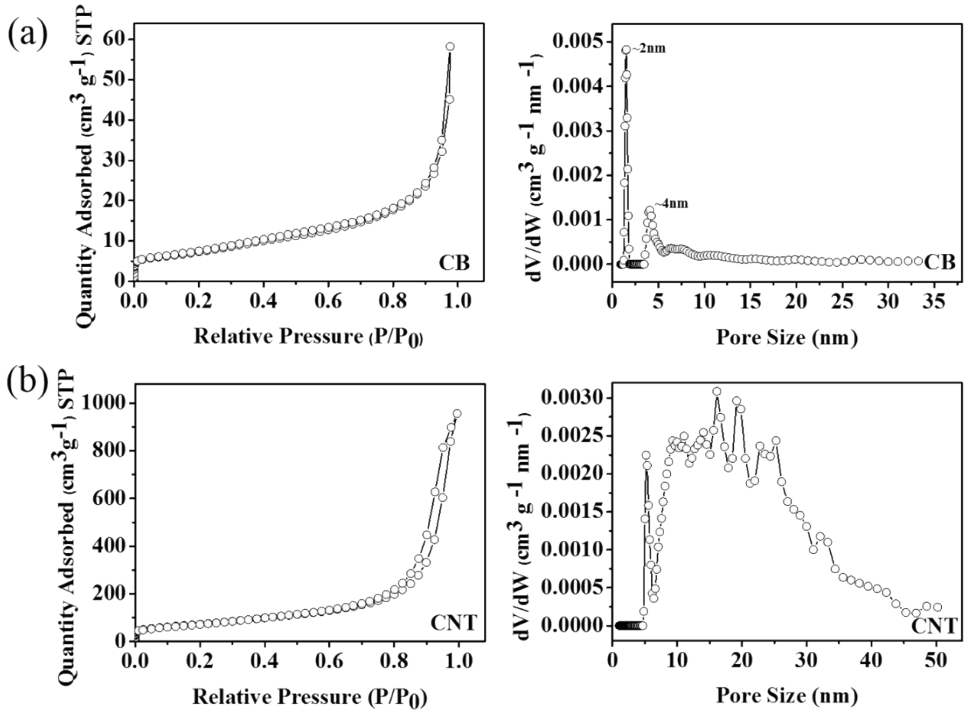

Fig. S2. N_2 adsorption-desorption isotherm and the pore size distribution of the (a) CB and (b) CNT.

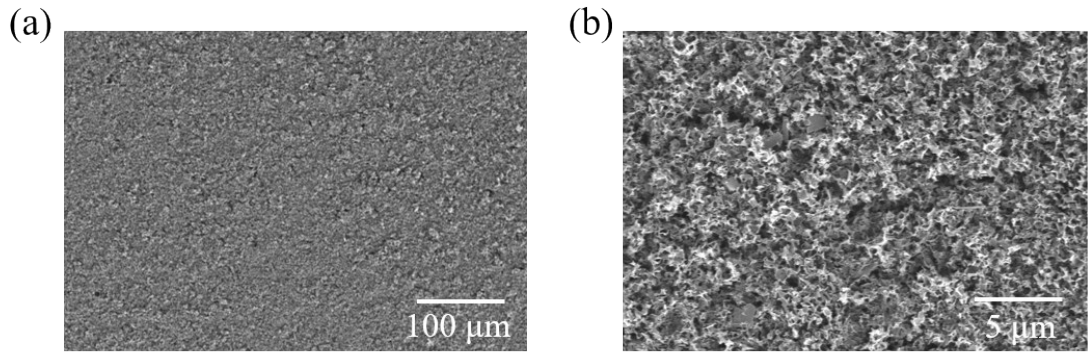

Fig. S3. The SEM images of N-GCs modification with (a) 100 μm and (b) 5μm.

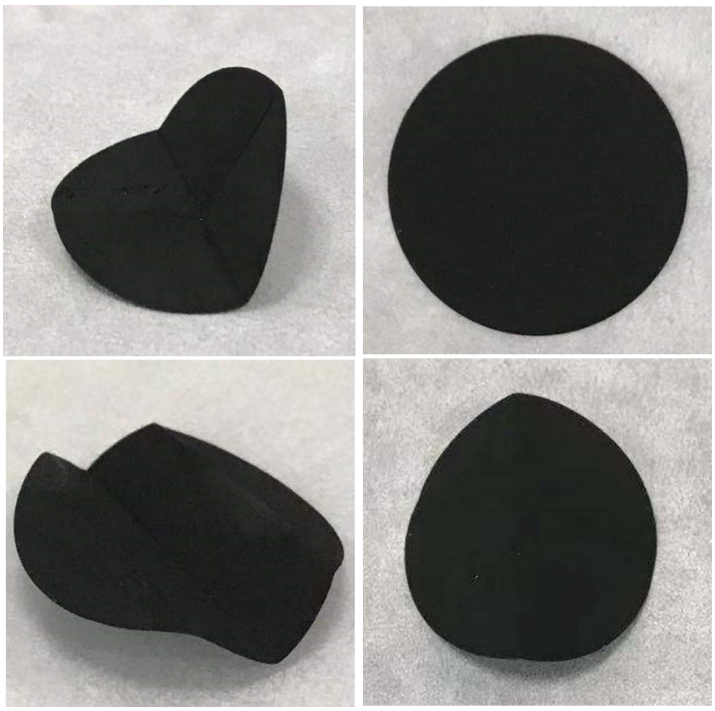

Fig. S4. Optical photographs for the N-GCs folded in different directions.

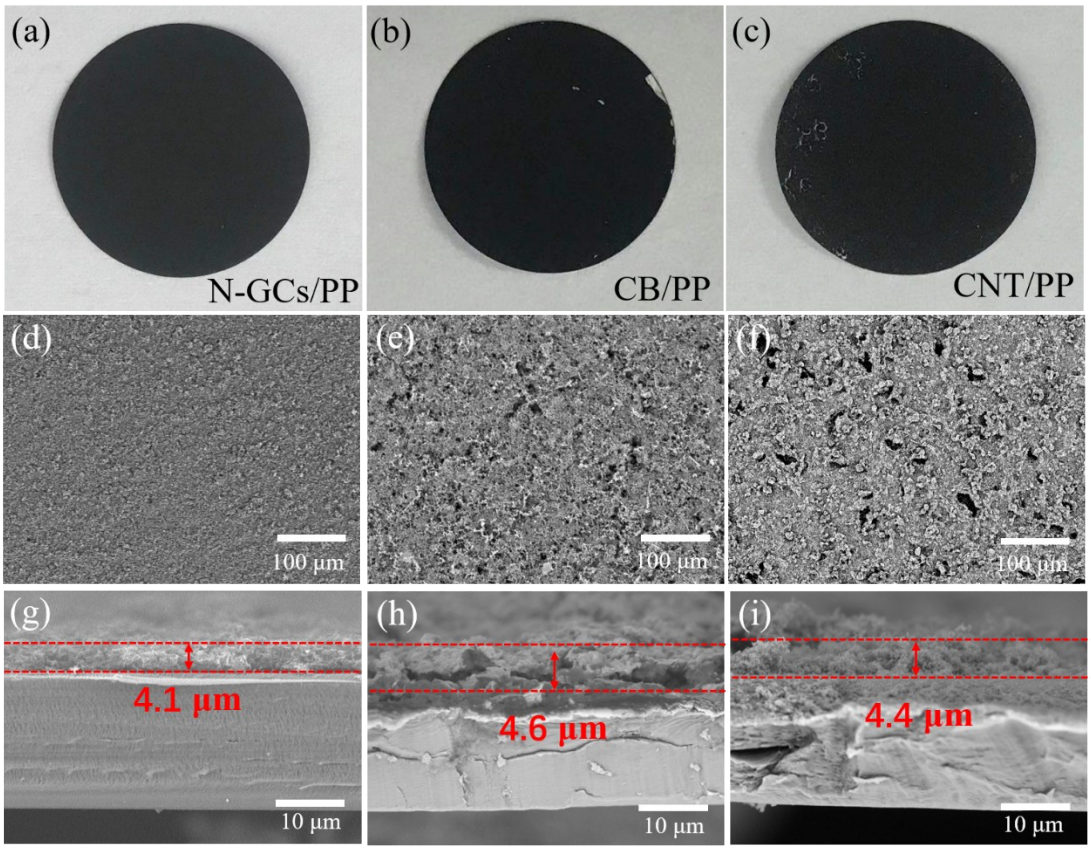

Fig. S5. Optical photographs, SEM images of the cathode-side and cross-section SEM images for (a), (d) and (g) N-GCs/PP, (b), (e) and (h) CB/PP, (c), (f) and (i) CNT/PP.

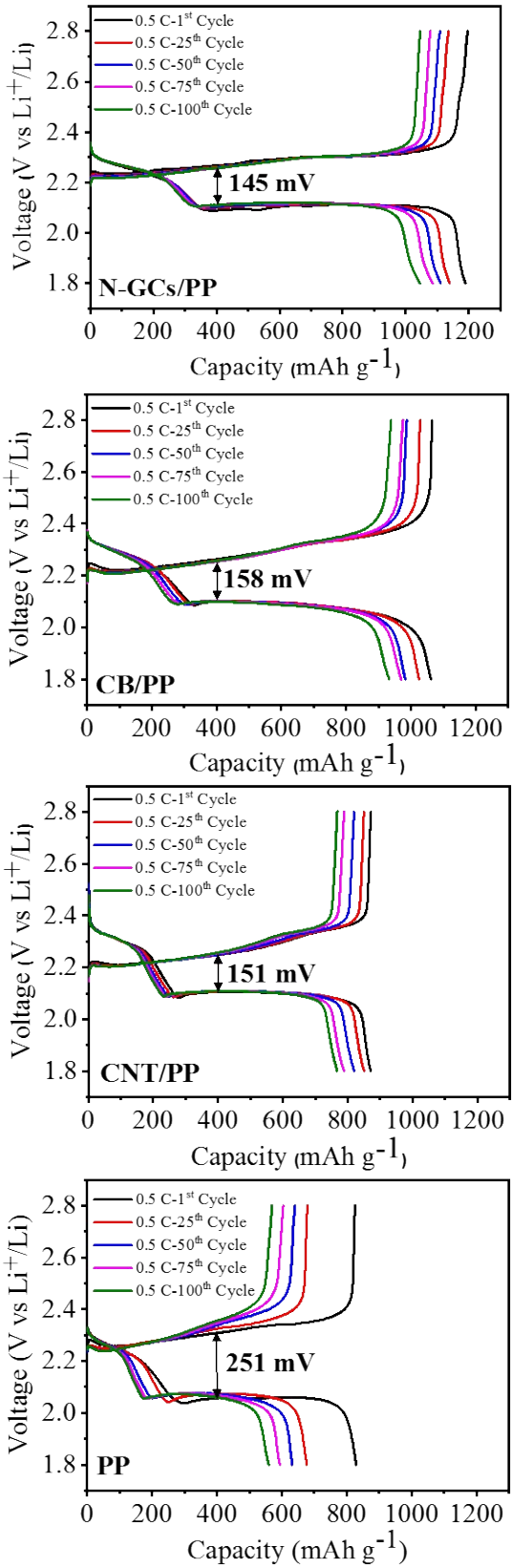

Fig. S6. The charge/discharge curves at current rate of 0.5 C for (a) N-GCs/PP cell, (b) CB/PP cell, (c) CNT/PP cell, and (d) PP cell.

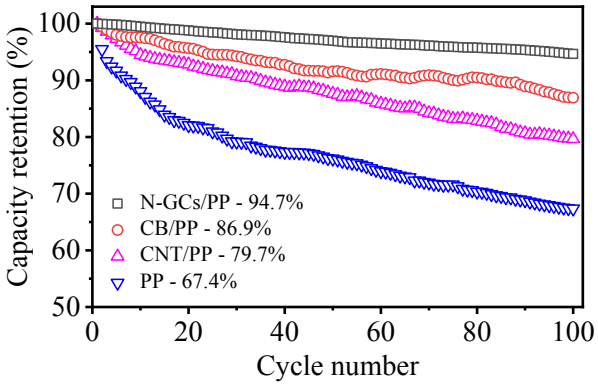

Fig. S7. The capacity retention of the upper discharge voltage plateaus for the N-GCs/PP, CB/PP, CNT/PP, and PP four cells at 0.5 C.

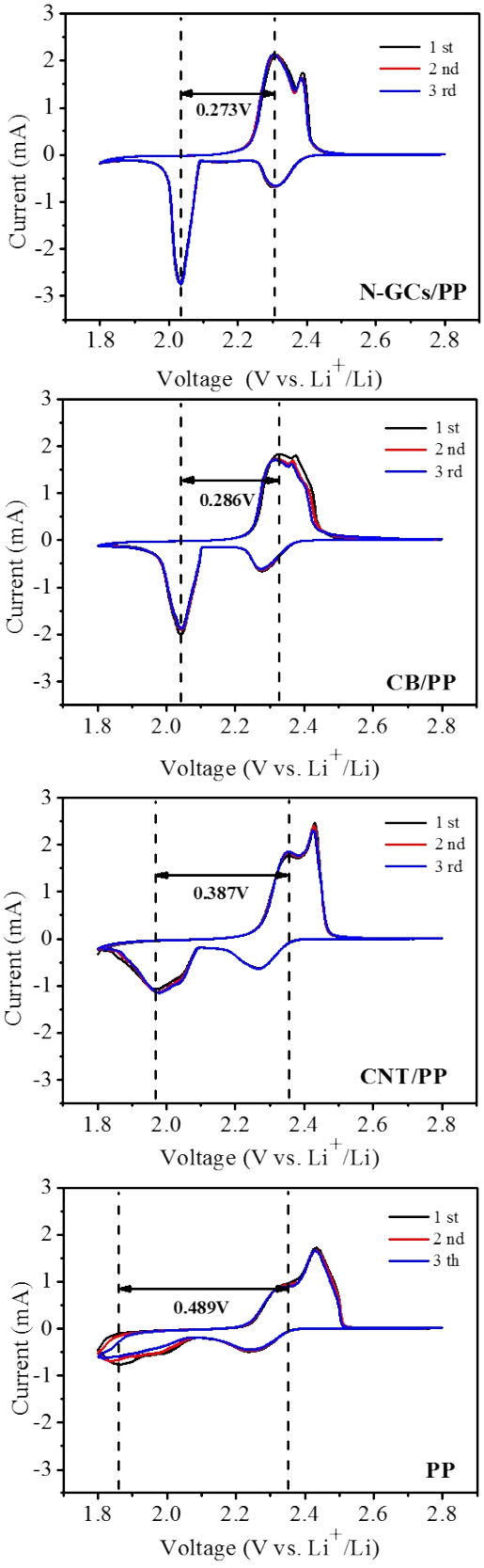

Fig. S8. The CV curves cycles at a scan rate of 0.1 mV s-1 for (a) N-GCs/PP cell, (b) CB/PP cell, (c) CNT/PP cell, and (d) PP cell. (first cycle sieved)

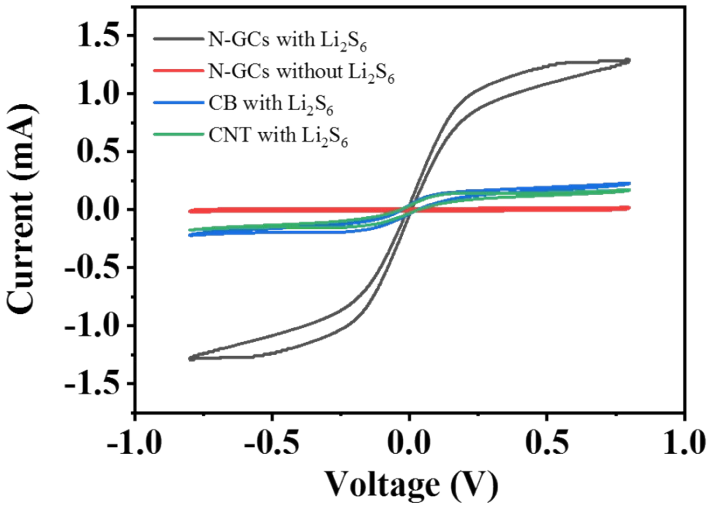

Fig. S9. The CV curves cycles of symmetric cells for N-GCs with Li_2S_6, N-GCs without Li_2S_6, CB with Li_2S_6, CNT with Li_2S_6 at a scan rate of 5 mV s^{-1}.

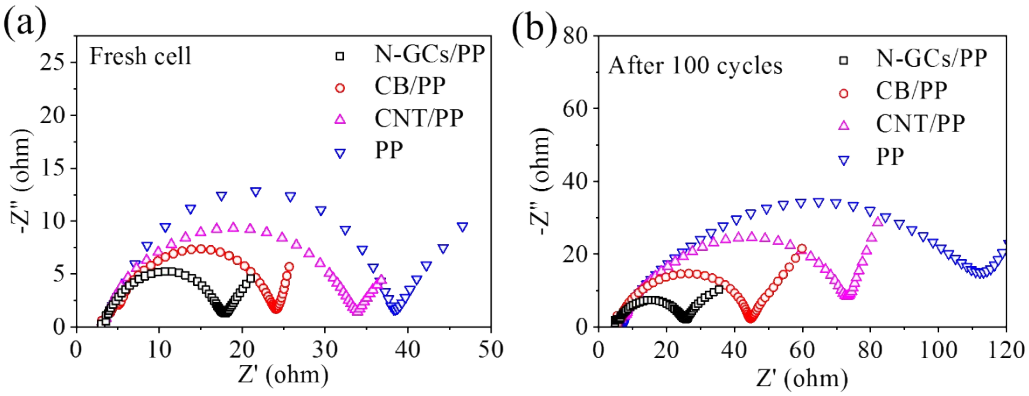

Fig. S10. The Nyquist plots of all four cells. (a) before cycling and (b) after 100 cycles at current rate of 0.5 C.

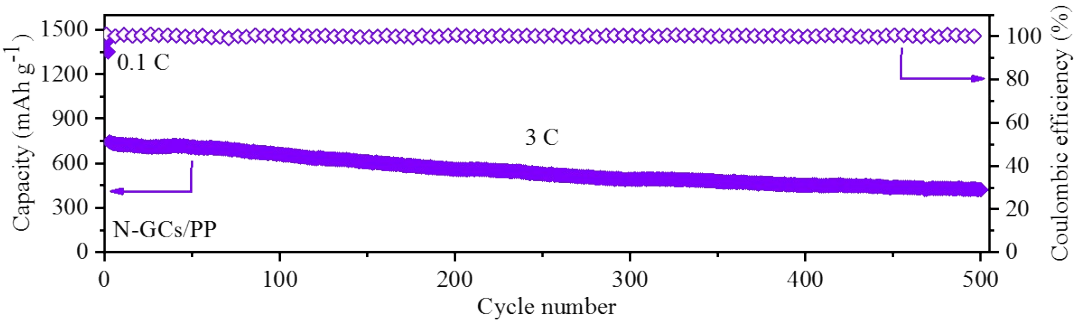

Fig. S11. Cycle performances of the N-GCs/PP at 3C.

Table S1. Comparison of the capacity maintained at various high current density in this work with the recently reported Li-S batteries[1-20].

Barrier	Coated mass ($mg\ cm^{-2}$)	Thickness (μm)	Initial capacity ($mAh\ g^{-1}$)	Cycles	Capacity ($mAh\ g^{-1}$)	Fading rate (% per cycle)	Ref
AB-CoS_2	0.5~0.7	12	618 at 2C	450	380	0.09	S1
SnS_2	0.6	/	1300 at 0.2C	150	1040	0.13	S2
B-rGO	0.2–0.3	25	1227.8 at 0.1C	300	663.6	0.15	S3
AB-SO_3^-	0.13	6	1262 at 0.1C	100	955	0.24	S4
CNF-VS_4	0.2–0.4	/	1135 at 0.2C	400	700	0.095	S5
N-MIMEC	0.2	4	1301 at 0.1C	100	971.3	0.25	S6
CAF	/	28	1096 at 0.2C	100	760.4	0.3	S7
LLZTO	/	5.5	649 at 0.5C	500	537	0.034	S8
PPy nanotube	1	20	1110.4 at 0.5C	300	801.6	0.092	S9
CCF	0.3	3	1215 at 0.5C	250	873.5	0.11	S10
G-LTO	0.346	35	801 at 1C	500	697	0.025	S11
PG	0.54	10	1165 at 0.5C	150	877	0.16	S12
mesoC	0.5	27	1378 at 0.2C	100	1021	0.25	S13
PP/GO/Nafion	0.053	/	1057 at 0.5C	200	969	0.042	S14
CoP nanosphere	0.2	15.37	928 at 1C	500	550	0.078	S15
CoP/C nanocube	0.3	17.7	938 at 1 C	500	562	0.08	S16
KBN	0.43	/	962.4 at 0.2C	150	846.9	0.08	S17
VS4/G	/	22.5	1000.0 at 0.5C	500	700	0.06	S18
MnS/CNF	0.59	24	1080 at 0.5C	100	894	0.17	S19
PVDF-HFP+CNF	1.87	20	1030 at 0.5C	500	556.2	0.092	S20
N-GC	**0.075**	**6.5**	**1169 at 1C**	**500**	**845.3**	**0.055**	**This work**

Table S2. Productivity of PVP

Sample	Mass before Carbonization (g)	Mass after Carbonization (g)	Productivity (%)
1	0.1585	0.0399	25.2%
2	0.1249	0.0309	24.7%
3	0.1752	0.0448	25.6%
4	0.1476	0.0361	24.5%
5	0.1552	0.0405	26.1%
6	0.1263	0.0336	26.6%
7	0.1638	0.0421	25.7%
8	0.1522	0.0379	24.9%

Table S3. BET surface area and pore volume of the N-GC nanosheets, CB and CNT.

Sample	BET surface area ($m^2\ g^{-1}$)	Total pore volume ($cm^3\ g^{-1}$)
N-GC	573.2	1.36
CB	25.5	0.062
CNT	249.6	1.31

[1] J. Balach, T. Jaumann, M. Klose, S. Oswald, J. Eckert, L. Giebeler, Adv. Funct. Mater. 25 (2015) 5285-5291.
[2] X. Chen, X. Ding, C. Wang, Z. Feng, L. Xu, X. Gao, Y. Zhai, D. Wang, Nanoscale 10 (2018) 13694-13701.
[3] X. Chen, Y. Huang, J. Li, X. Wang, Y. Zhang, Y. Guo, J. Ding, L. Wang, J. Colloid and Interface Sci. 559 (2020) 13-20.
[4] J. Lin, K. Zhang, Z. Zhu, R. Zhang, N. Li, C. Zhao, ACS Appl. Mater. Interfaces (2019).
[5] G. Ma, F. Huang, Z. Wen, Q. Wang, X. Hong, J. Jin, X. Wu, J. Mater. Chem. A 4 (2016) 16968-16974.
[6] B. Moorthy, S. Kwon, J.-H. Kim, P. Ragupathy, H.M. Lee, D.K. Kim, Nanoscale Horiz. 4 (2019) 214-222.
[7] H. Qu, J. Ju, B. Chen, N. Xue, H. Du, X. Han, J. Zhang, G. Xu, Z. Yu, X. Wang, G. Cui, J. Mater. Chem. A, 6 (2018) 23720-23729.
[8] M. Rana, M. Li, Q. He, B. Luo, L. Wang, I. Gentle, R. Knibbe, J. Energy Chem. 44 (2020) 51-60.
[9] H. Shao, F. Ai, W. Wang, H. Zhang, A. Wang, W. Feng, Y. Huang, J. Mater. Chem. A 5 (2017) 19892-19900.
[10] H. Shao, B. Huang, N. Liu, W. Wang, H. Zhang, A. Wang, F. Wang, Y. Huang, J. Mater. Chem. A 4 (2016) 16627-16634.
[11] M. Wang, L. Fan, Y. Qiu, D. Chen, X. Wu, C. Zhao, J. Cheng, Y. Wang, N. Zhang, K. Sun, J. Mater. Chem. A, 6 (2018) 11694-11699.
[12] X. Wang, X. Zhao, C. Ma, Z. Yang, G. Chen, L. Wang, H. Yue, D. Zhang, Z. Sun, J. Mater. Chem. A (2020).
[13] F. Wu, J. Qian, R. Chen, Y. Ye, Z. Sun, Y. Xing, L. Li, J. Mater. Chem. A 4 (2016) 17033-17041.
[14] F. Zeng, Z. Jin, K. Yuan, S. Liu, X. Cheng, A. Wang, W. Wang, Y.-s. Yang, J. Mater. Chem. A, 4 (2016) 12319-12327.
[15] P. Zeng, L. Huang, X. Zhang, Y. Han, Y. Chen, Appl. Surface Sci. 427 (2018) 242-252.
[16] P.-Y. Zhai, H.-J. Peng, X.-B. Cheng, L. Zhu, J.-Q. Huang, W. Zhu, Q. Zhang, Energy Storage Mater. 7 (2017) 56-63.
[17] A. Zhang, X. Fang, C. Shen, Y. Liu, I.G. Seo, Y. Ma, L. Chen, P. Cottingham, C. Zhou, Nano Research 11 (2018) 3340-3352.
[18] Y. Zhang, G. Xu, Q. Kang, L. Zhan, W. Tang, Y. Yu, K. Shen, H. Wang, X. Chu, J. Wang, S. Zhao, Y. Wang, L. Ling, S. Yang, J. Mater. Chem. A 7 (2019) 16812-16820.
[19] Y. Zhao, M. Liu, W. Lv, Y.-B. He, C. Wang, Q. Yun, B. Li, F. Kang, Q.-H. Yang, Nano Energy 30 (2016) 1-8.
[20] T.Z. Zhuang, J.Q. Huang, H.J. Peng, L.Y. He, X.B. Cheng, C.M. Chen, Q. Zhang, Small 12 (2016) 381-389.